

Supplement of Atmos. Chem. Phys., 20, 14523–14545, 2020  
<https://doi.org/10.5194/acp-20-14523-2020-supplement>  
© Author(s) 2020. This work is distributed under  
the Creative Commons Attribution 4.0 License.



*Supplement of*

## **Measurement report: Aircraft observations of ozone, nitrogen oxides, and volatile organic compounds over Hebei Province, China**

**Sarah E. Benish et al.**

*Correspondence to:* Sarah Benish (sebenish@umd.edu)

The copyright of individual parts of the supplement might differ from the CC BY 4.0 License.

## Supplemental Material

5

10

### 15 **Text S1**

We exclude two WAS canisters from this analysis due to evidence of contamination. The first sample was collected on May 21 at 399 m pressure altitude. This sample was heavily polluted with i-butane (25.8 ppbv), i-pentane (57.7 ppbv), as well as longer chain alkanes like 2,3-dimethylbutane (4.2 ppbv), 2-methylpentane (5.9 ppbv), cyclopentane (2.7 ppbv), 2-methylheptane (16.1 ppbv), and 3-methylpentane (3.5 ppbv) in addition to aromatics like toluene (41.3 ppbv) and benzene (20.8 ppbv). Many of these compounds are typical of fuel evaporation or from petrochemical industries, indicating this canister may have directly sampled directly in the plume of one of these sources. Since this study is primarily focused with evaluating aloft VOCs away from their direct emission sources, the data from this canister were removed from this analysis.

25 The second contaminated sample was collected on May 28 at 3:36 UTC. This sample was filled to ambient pressure at 3000 m in relatively clean air, based on *in situ* observations at the time the canister was collected (CO=111 ppbv, CH<sub>4</sub>=1890 ppbv, CO<sub>2</sub>=406 ppmv, O<sub>3</sub>=84 ppbv). The concentrations of VOCs for this sample are outliers relative the associated abundances of the trace gases. This anomaly is indicative of valve leakage during transit or ambient air entering the WAS canister after the flight. The observed CO to acetylene ratio (ppbv/ppbv), often used as a tracer for the age of an air mass, was much smaller in this sample (70 ppbv/ppbv) compared to other samples collected at a similar altitude (~400 ppbv/ppbv).

30

**Table S1. Summary statistics of the 1-second measured concentrations for O<sub>3</sub>, NO<sub>2</sub>, and CO, flight path descriptions, and weather conditions for each flight during ARIAs. Negative values of NO<sub>2</sub> indicate when the instrument was measuring around the detection limit.**

Date (DOY)	Takeoff (LST)	Landing (LST)	Mean O <sub>3</sub> (Range), ppbv	Mean NO <sub>2</sub> (Range), ppbv	Mean NO <sub>y</sub> (Range), ppbv	Mean CO (Range), ppbv	Flight Description	Weather Conditions
May 8 (129)	10:30	14:32	76.6 (62.7-83.9)	No data	15.6 (9.0-29.4)	No data	Spirals over Julu (400-3500 m) at 10:58 LST, Quzhou (350-3500 m) at 12:00 LST, Xingtai (400-3000 m) at 12:23 LST, and Shijiazhuang (100-3500 m) at 14:05.	A high over the region and a weak low to the NE moving to the E. Strong S winds in daytime (surface wind speed up to 10 m/s). Cold front passed 2 days prior.
May 15 (136)	12:17	15:04	64.6 (54.4-85.8)	No data	No data	No data	Spirals over Julu (400-3500 m) at 12:43 LST and Quzhou at 13:41.	A high over the region and an occluded front to the E over the Yellow Sea. Surface winds mostly from the NE up to 10 m/s.
May 16 (137)	15:03	15:54	85.3 (70.5-96.0)	No data	22.8 (6.1-29.6)	No data	Flight to the southeast to the W of Julu. Flight altitude about 400 m.	A high over the region and a cold front to the E of the Korean Peninsula. Morning surface winds from the W (< 8 m/s) with a shift late-morning from the SE (< 10 m/s).
May 17 (138)	8:21	11:13	80.1 (45.0-99.1)	8.8 (-0.1-38.4)	30.2 (0.2-89.7)	590.5 (114.3-6053.6)	Low altitude transect to Julu, with spirals at Julu (650-2800 m) at 9:47 LST and Quzhou (400-3000 m) at 10:19 LST.	Surface high pressure conditions throughout the region and low pressure to the N and W. A 700 hPa ridge is situated over North Korea. Surface W winds in the morning (< 5 m/s) with a shift in late-morning from the SE (< 10 m/s).
May 19 (140)	15:42	17:09	97.1 (75.4-130.2)	1.4 (-0.1-6.8)	11.3 (3.6-29.1)	131.4 (90.8-540.0)	Spirals over the airport.	Weak surface high pressure conditions over the region and low pressure systems over S Mongolia and Inner Mongolia. Upper level 700 hPa trough from the previous day moved E to Sea of Okhotsk. Surface winds from the W in the morning (< 5 m/s) with a shift in late-morning from the SE (< 7 m/s).
May 21 (142)	11:57	13:41	99.5 (67.1-145.6)	1.9 (-0.1-16.4)	No data	238.5 (80.5-564.5)	Flew to southeast at low altitude (1000 m) to a point (114.9 °E, 37.6 °N). Spirals over Quzhou (300-3000 m) at 12:40 LST and Xingtai (300-2400 m) at 13:34 LST.	Weak surface high pressure conditions over the region with a Siberian anticyclone to the N. Surface winds from the W in the morning with a shift in late-morning from the E (< 6 m/s).
May 28 (149)	10:16 16:29	13:26 18:24	86.3 (63.5-100.3); 88.9 (72.9-112.3)	3.2 (-0.1-27.0); 2.6 (0.01-10.4)	No data	332.2 (97.1-1264.9); 215.2 (88.1-963.3)	Morning flight flew spirals over Xingtai (350-3000 m) at 11:02 LST and Julu (450-2500 m) at 12:29 LST. During the afternoon flight, spirals over Xingtai (350-3000 m) at 16:57 LST.	High pressure over the region and a stationary front ~1000 km to the S near Shanghai. Surface winds mostly from the SE (< 5 m/s).
June 2 (154)	13:47	14:53	94.9 (79.6-106.3)	1.5 (-0.1-5.4)	24.3 (14.9-70.7)	256.7 (95.1-487.5)	Spirals over the airport.	High over the region with low pressure over central China and a stationary front to the S near Shanghai.

											Light surface winds (< 5 m/s) mostly from the W.
June 6 (158)	10:08	12:01	99.9 (67.5-134.7)	0.7 (-0.1-4.9)	No data	296.2 (105.1-573.2)	Low altitude (< 2000 m) spirals to the SE of Shijiazhuang. Spirals over Julu at 10:44 LST.	Several weak low pressure systems over the region. A stationary front is over the East China Sea. Variable winds less than 5 m/s.			
June 11 (163)	11:02	13:45	76.7 (57.2-90.8)	2.3 (-0.1-6.7)	16.9 (11.1-23.8)	187.4 (88.2-412.9)	Low altitude transect (2000 m) to NE Julu. Spirals over Xingtai (600-3000 m) at 11:54 LST and Shijiazhuang (600-3000 m) at 13:12 LST.	Low pressure over region with a Siberian anticyclone over Mongolia. A stationary front is located to the S near Taiwan. Variable surface winds, with the strongest winds (12 m/s) from the N in the morning.			

**Table S2. Summary statistics of alkanes, alkenes/alkynes, and aromatics quantified for all WAS canisters (pptv), as well as the method detection limit (MDL, in pptv), rate constants with OH (kOH), maximum incremental reactivity (MIR) value, and ratio to CO (pptv/ppbv) for compounds with R>0.50. Values less than 1 pptv are not shown.**

35

	Mean (STD)	Min	5 <sup>th</sup>	25 <sup>th</sup>	50 <sup>th</sup>	75 <sup>th</sup>	95 <sup>th</sup>	Max	MDL <sup>†</sup>	kOH <sup>‡</sup>	MIR <sup>†</sup>	Ratio to CO (pptv/ppbv)
<b>Alkanes</b>												
Ethane	2648 (710)	1804	1902	203 3	2525	2998	4066	4154	50	$6.90 \times 10^{-12} \times e^{-1000/T}$	0.28	2.5
Propane	1391 (231)	978	1044	119 6	1356	1509	1769	1887	21	$7.60 \times 10^{-12} \times e^{-585/T}$	0.49	-
n-Butane	363 (278)	83	92	207	259	480	1131	1210	30	$9.80 \times 10^{-12} \times e^{-425/T}$	1.15	-
2,2-Dimethylbutane	13 (14)	2	3	5	9	17	42	64	7	$3.22 \times 10^{-11} \times e^{-781/T}$	1.17	-
2,3-Dimethylbutane	44 (93)	2	2	5	11	27	293	400	5	$1.24 \times 10^{-17} \times T^2 \times e^{-585/T}$	0.97	-
i-Butane	624 (997)	56	70	109	246	673	3546	3963	29	$1.16 \times 10^{-17} \times T^2 \times e^{225/T}$	1.23	-
n-Pentane	119 (113)	19	26	54	71	155	400	479	5	$2.44 \times 10^{-17} \times T^2 \times e^{183/T}$	1.31	-
i-Pentane	674 (1255)	32	48	118	168	413	3785	5444	12	$3.70 \times 10^{-12}$	1.45	-
Cyclopentane	34 (64)	2	2	5	12	25	168	296	26	$2.67 \times 10^{-11} \times e^{-590/T}$	2.39	-
Methylcyclopentane	26 (29)	2	3	7	15	28	91	115	8	$7.66 \times 10^{-12}$	2.19	-
2-Methylpentane	111 (144)	8	11	39	61	103	363	667	5	$5.30 \times 10^{-12}$	1.5	-
3-Methylpentane	53 (88)	3	3	9	26	55	224	395	7	$5.40 \times 10^{-12}$	1.8	-
2,3-Dimethylpentane	27 (33)	4	4	9	19	26	86	152	4	$1.95 \times 10^{-11} \times e^{-330/T}$	1.34	-
2,4-Dimethylpentane	31 (53)	3	3	6	11	25	137	228	5	$2.49 \times 10^{-11} \times e^{-443/T}$	1.55	-
2,2,4-Trimethylpentane	433 (1117)	9	11	28	57	236	2120	5422	3	$2.09 \times 10^{-12} \times \left(\frac{T}{298}\right)^{2.00} \times e^{140/T}$	1.26	-
2,3,4-Trimethylpentane	232 (652)	9	9	15	33	96	987	3253	8	$9.85 \times 10^{-12} \times e^{-124/T}$	1.03	-
n-Hexane	123 (180)	6	8	24	46	130	541	699	16	$1.53 \times 10^{-17} \times T^2 \times e^{414/T}$	1.24	-
Cyclohexane	15 (13)	1	2	5	9	27	44	44	16	$2.88 \times 10^{-17} \times T^2 \times e^{-309/T}$	1.25	-
Methylcyclohexane	17 (23)	3	5	6	10	14	54	114	8	$1.18 \times 10^{-11}$	1.70	-
2-Methylhexane	39 (72)	6	8	13	18	27	147	362	8	$6.86 \times 10^{-12}$	1.19	-
3-Methylhexane	44 (88)	7	7	12	16	33	178	438	6	$7.15 \times 10^{-12}$	1.61	-

n-Heptane	41 (52)	9	12	16	22	39	142	255	7	$1.59 \times 10^{-17} \times T^2 \times e^{478/T}$	1.07	-
2-Methylheptane	399 (1106)	11	13	32	63	172	1718	5515	8	$2.51 \times 10^{-17} \times T^2 \times e^{447/T}$	1.07	-
3-Methylheptane	15 (13)	7	7	8	11	14	56	59	9	$2.51 \times 10^{-17} \times T^2 \times e^{447/T}$	1.24	-
Octane	26 (19)	10	10	15	23	29	59	102	12	$2.76 \times 10^{-17} \times T^2 \times e^{378/T}$	0.90	-
n-Nonane	22 (12)	13	14	15	17	25	39	72	21	$2.51 \times 10^{-17} \times T^2 \times e^{447/T}$	0.78	-
n-Decane	58 (57)	14	14	24	38	76	155	288	10		0.68	
<b>Alkenes/Alkynes</b>												
Acetylene	803 (465)	234	284	454	578	1175	1506	1934	48	$1.69 \times 10^{-12} \times e^{-233/T}$	0.95	1.4
Ethylene	884 (923)	185	191	281	405	1093	2941	3536	30	$2.14 \times 10^{-12} \times e^{411/T}$	9.00	2.9
Propylene	168 (44)	102	104	143	164	199	223	308	25		11.66	-
1-Butene	23 (10)	10	11	17	19	25	43	46	30	$6.60 \times 10^{-12} \times e^{465/T}$	9.73	-
cis-2-Butene	3 (6)	-	-	1	1	2	7	31	23	$1.10 \times 10^{-11} \times e^{487/T}$	14.24	-
trans-2-Butene	3 (3)	-	-	1	2	4	9	16	31	$1.01 \times 10^{-11} \times e^{550/T}$	15.16	-
Isoprene	35 (39)	2	5	8	20	37	117	138	15	$2.70 \times 10^{-11} \times e^{390/T}$	10.61	-
1-Pentene	8 (3)	4	4	6	7	9	14	18	9	$5.86 \times 10^{-12} \times e^{500/T}$	7.21	-
cis-2-Pentene	2 (3)	-	-	1	1	2	4	16	8	$6.54 \times 10^{-11}$	10.38	-
trans-2-Pentene	2 (3)	-	-	1	1	2	12	14	8	$6.69 \times 10^{-11}$	10.56	-
1-Hexene	6 (5)	3	3	4	5	6	9	27	11	$3.70 \times 10^{-11}$	5.49	-
<b>Aromatics</b>												
Benzene	510 (521)	63	96	188	330	570	1819	2183	7	$2.30 \times 10^{-12} \times e^{-190/T}$	0.72	1.8
Toluene	757 (1188)	31	43	159	300	627	4064	4402	5	$1.80 \times 10^{-12} \times e^{340/T}$	4.00	-
Styrene	14 (12)	4	4	6	8	18	43	45	13	$5.80 \times 10^{-11}$	1.73	-
m/p-Xylene	108 (155)	16	22	43	62	117	345	789	2	$1.87 \times 10^{-11}$	7.80	-
o-Xylene	43 (51)	8	11	17	28	44	119	263	3	$1.36 \times 10^{-11}$	7.64	-
Ethylbenzene	73 (85)	12	15	27	45	83	198	423	3	$7.00 \times 10^{-12}$	3.04	-
Isopropylbenzene	15 (8)	7	7	10	13	18	28	48	20	$6.61 \times 10^{-12}$	2.52	0.02
n-Propylbenzene	15 (20)	4	4	7	10	15	37	104	16	$5.80 \times 10^{-12}$	2.03	0.06
2-Ethyltoluene	14 (17)	5	5	7	9	13	35	89	10	$1.86 \times 10^{-11}$	5.59	0.05
3-Ethyltoluene	19 (18)	4	5	9	13	18	59	88	20	$1.18 \times 10^{-11}$	7.39	0.05
4-Ethyltoluene	19 (26)	4	4	7	11	18	60	132	20	$1.19 \times 10^{-11}$	4.44	0.07
1,3-Diethylbenzene	20 (28)	4	4	6	8	12	64	248	10	$1.86 \times 10^{-11}$	7.10	0.15
1,4-Diethylbenzene	27 (40)	8	8	11	18	22	53	218	10	$1.18 \times 10^{-11}$	4.43	0.12
1,2,3-Trimethylbenzene	18 (24)	7	7	9	13	16	43	130	2	$3.27 \times 10^{-11}$	11.97	0.07
1,2,4-Trimethylbenzene	30 (30)	8	9	15	23	31	65	160	3	$3.25 \times 10^{-11}$	8.87	0.08
1,3,5-Trimethylbenzene	10 (11)	3	3	4	6	8	28	54	4	$5.67 \times 10^{-11}$	11.76	-

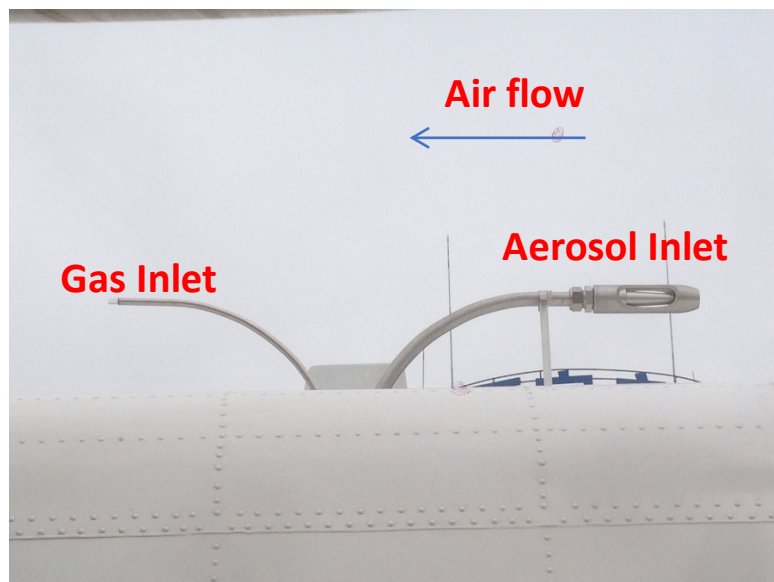
\* TO-15 method, where the standard deviation of seven replicates near the detection limit are multiplied by 3.14 (Student's t value with 99% confidence).

‡ Reaction rate coefficient with OH.

40 † Maximum Incremental Reactivity (MIR, units=g O<sub>3</sub>/g VOC), from Carter, (2010).

Figure S1. Left: Picture of the gas (alt-facing) and aerosol inlet (forward facing) on top of the Y-12 aircraft. Right: Picture of the Cloud Water Inertial Probe (CWIP) on the Y-12 aircraft installed under the port wing.

45



50

55

60

65

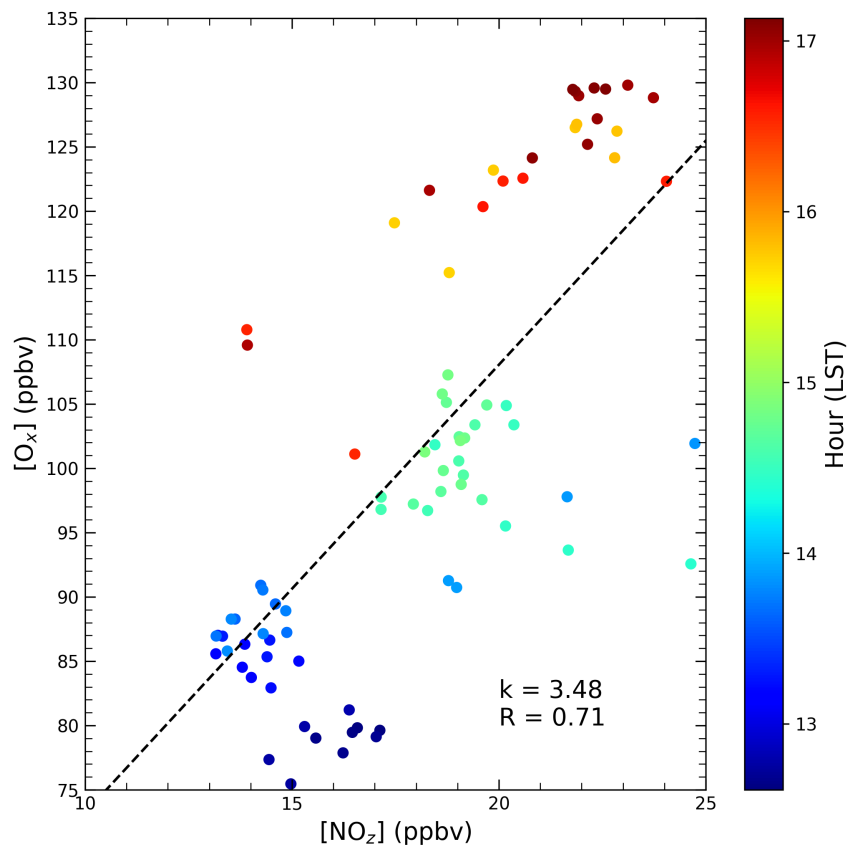
70

75

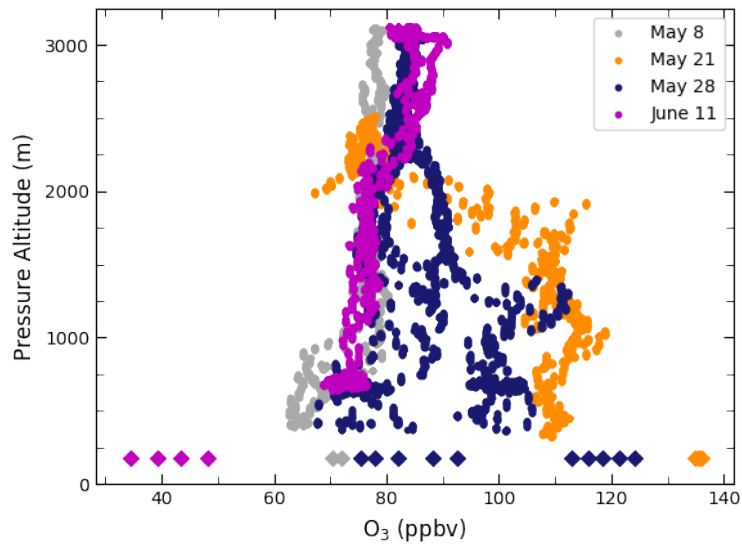
80

Figure S2. Scatter plot of 1-minute average  $O_x$  ( $O_3+NO_2$ ) as a function of  $NO_z$  ( $NO_y-NO_x$ ) less than 30 ppbv below 1500 m. The color shows the local hour of collection. The line is the linear regression with the slope ( $k$ ) and Pearson R correlation coefficient.

85



90 **Figure S3. Vertical profiles (N=19) of 1-second O<sub>3</sub> concentrations (ppbv) from the Y-12 (circles) compared to concurrent average concentrations measured at the A<sup>2</sup>BC site in Xingtai (diamonds). The average surface O<sub>3</sub> concentration was computed by averaging the 5-minute data interval starting 30 minutes before the spiral until 30 minutes after the spiral was completed.**



95

100

105

Figure S4. Scatter plot of 1-second CO (ppbv) and CO<sub>2</sub> (ppmv) (left) and SO<sub>2</sub> (ppbv) and CO<sub>2</sub> (right) sampled during a plume over Julu on June 6.

